

STREAM

IST-1999-10341

STREAM CONSORTIUM:

**CNR-LAMEL / ST Microelectronics / ISEN / SOFT IMAGING SYSTEM /
University of Sheffield / IMEC / CNR-IESS / University of Perugia**

DELIVERABLE D21

Workpackage WP3

Lead participant: CNR-IESS

Determination of strain tensor values on test structures with different dimension by XRD and comparison with TEM/CBED, microRS and process simulation

<i>Main Author</i>	S. Lagomarsino, CNR-IESS		
<i>Contributing authors</i>	A. Cedola, CNR-IESS; F. Scarinci, CNR-IESS; C. Giannini, CNR-IC; A. Guagliardi, CNR-IC;		
<i>Date:</i>	15-04-2002	<i>Doc.No:</i>	IST10341-IE-RP002
<i>Keywords:</i>	X-ray micro-diffraction, Waveguide, Strain measurement, Synchrotron radiation		

<p><i>Distribution list</i></p>	<p>Project Officer: B.Netange (3 copies)</p> <p>All Partners:</p> <p>A. Armigliato CNR-LAMEL</p> <p>G.P.Carnevale ST Microelectronics</p> <p>V. Senez ISEN</p> <p>T. Schilling Soft Imaging System</p> <p>A.G.Cullis USFD (University of Sheffield)</p> <p>I. De Wolf IMEC</p> <p>G. Carlotti UniPg (University of Perugia)</p>

Table of contents

Abstract	p. 4
1. Improved experimental procedures	p. 4
2. The instrument for microdiffraction	p. 6
3. Software for data analysis	p. 11
4. Results of measurements	p. 17
5. Conclusions	p. 21

Abstract

This deliverable presents the conclusions of the work on the new x-ray microdiffraction method aimed at measuring local deformation of crystalline structure. The main features of the technique has been presented in deliverable D11, where the instrument installed at the beamline ID13 has been described. In the workplan the present deliverable should contain only the result of the microstrain determination on test structures, and the comparison with the other characterisation techniques and the simulation, but in the course of the project we realised some important aspects that pushed us to improve both the instrumentation and the experimental procedures. We will describe these aspects in parts 1) and 2) of this deliverable. Part 3 will present in detail the data analysis programme, and part 4) the result of the measurements together with the comparison. Finally, part 5) will end this deliverable with final comments and conclusions.

1. Improved experimental procedures

The experience acquired in the course of the first year of STREAM activity pushed us to recognise that the strain sensitivity could be significantly improved adding a second monochromator. We recall here that we used the properties of the waveguide to obtain high spatial resolution in the vertical plane, while maintaining the incident beam characteristics in the horizontal plane which contain the incident and diffracted beams. In these conditions, since the beamline monochromator disperses in the vertical plane, diffraction in the horizontal plane suffers of the angular dispersion due to the energy band width (of the order of 10^{-4}). The angular dispersion limits the strain sensitivity to few parts in 10^{-4} , and has also some influence on the determination of larger strain if the volume interested is small. To overcome this limitation we put a second monochromator which disperses in the horizontal plane in order to achieve a double crystal parallel geometry.

Fig. 1.1 shows in a schematic way the main difference between the two set-ups.

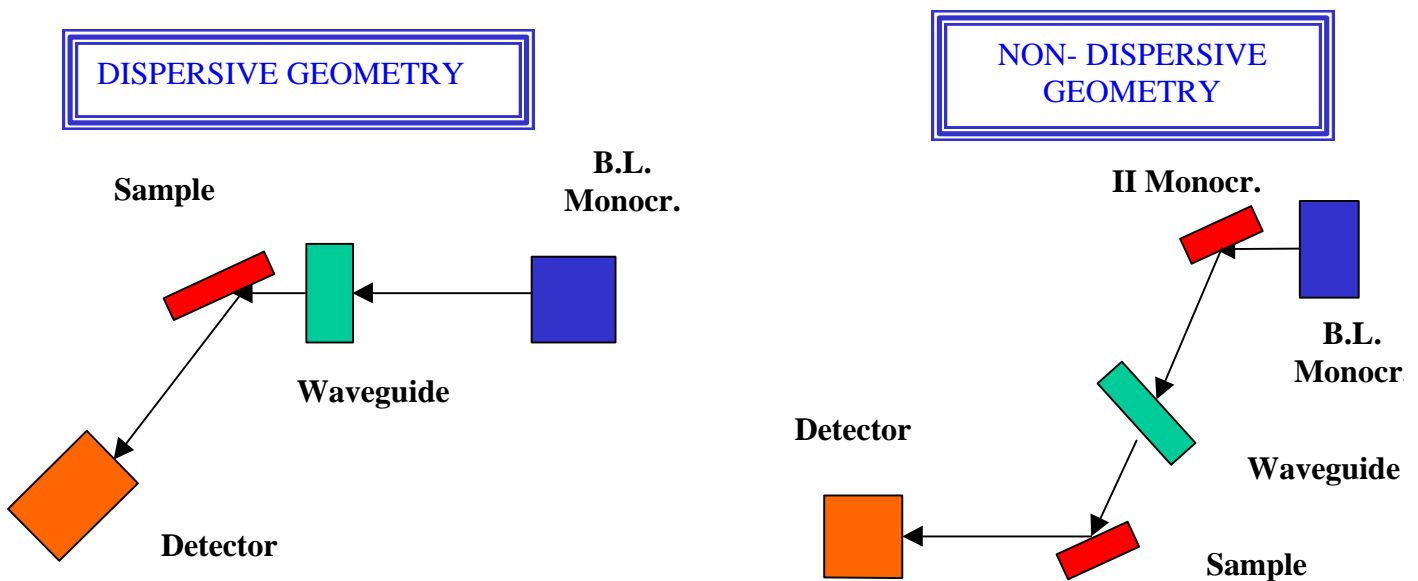


Figure 1.1: Schematic difference between dispersive and non-dispersive geometry

Fig.1.2 shows the comparison between a diffraction profile taken in a non-dispersive and dispersive geometry. It is evident the reduction in width and in the intensity of the tails of the non-dispersive geometry., allowing a better sensitivity to strain.

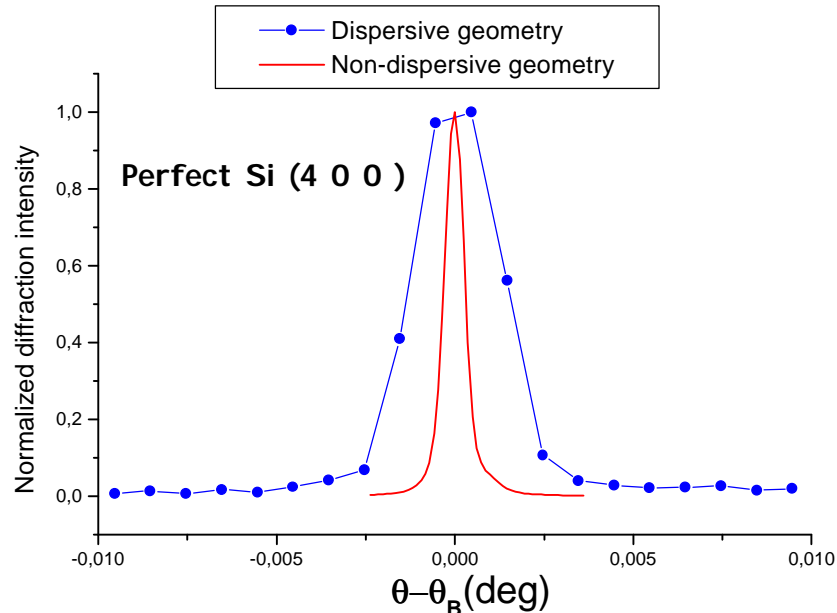


Figure 1.2: Comparison between a diffraction profile taken in a non-dispersive and dispersive geometry.

A draw-back in using the non-dispersive arrangement is a reduction in intensity of about a factor 5. This implies severe problems to use a CCD camera which is inherently less sensitive than an integrated detector as, for ex., an NaI scintillator. Therefore, with respect to the scheme presented in del. D11, instead to adopt a projection geometry that requires a CCD camera, we adopted a scanning geometry with the sample close to the waveguide exit and a standard scintillation detector. In this geometry we exploit the small beam dimensions provided by the waveguide: only a small portion of the sample is probed by the beam and the whole information requires a vertical translation of the sample. Since the beam from the waveguide has a divergence of the order of 1 mrad, the distance wg-sample must be taken as short as possible in order to have the smallest beam at the sample. Considering a distance of the order of 100-200 μ , the best spatial resolution that can be obtained in the scanning geometry is of the order of 300 nm. Taking into account the size of the structure of interest in this project, this means that we cannot distinguish between different parts of the same zone (for ex. between the centre and the edge of the active zone), but we can give a reliable value of the overall strain of the structure. Therefore the two geometries, projection or scanning, are in some way complementary one to the other, and the choice depends on the kind of structure to analyze, on the characteristics of the beamline and on the detector in use.

We described in del. D11 the measurement procedures and data processing in the case of the projection geometry. In the case of scanning the procedure is even simpler, because the different diffraction profiles (rocking curves) as a function of the vertical position of the sample are analyzed in sequence in order to reconstruct the whole variation of the local strain. If the angular region of the rocking curve is large, it could be necessary that also the detector, which in general carries horizontal and vertical slits, moves in synchronism with the sample describing what is known as a

θ - 2θ scan, i.e. a combined movement where for a given rotation angle of the sample the detector rotates around the sample of twice such an angle.

2) The instrument for microdiffraction

Several reasons pushed us in the course of the second year of activity of STREAM to design and build a new instrument for microdiffraction. First of all the instrument described in del. D11 is fixed at the beamline ID13 and property of ESRF. On other beamlines the experimental set-up was not so optimised for the x-ray waveguide, and required a quite long time of preparation. On the other side nearly all the beamlines at ESRF are heavily oversubscribed, and it can be very useful to have the opportunity to carry out experiments on several beamlines. Moreover, the ID13 beamline is specialised in soft condensed matter, and some aspects of the instrumentation for x-ray waveguides were mostly adapted to this aspect. For example, the insertion of a second monochromator would not be so straightforward on this installation. Another consideration is related to the alignment procedures. These are very delicate and time-consuming. Often a considerable fraction of beam time is wasted for them.

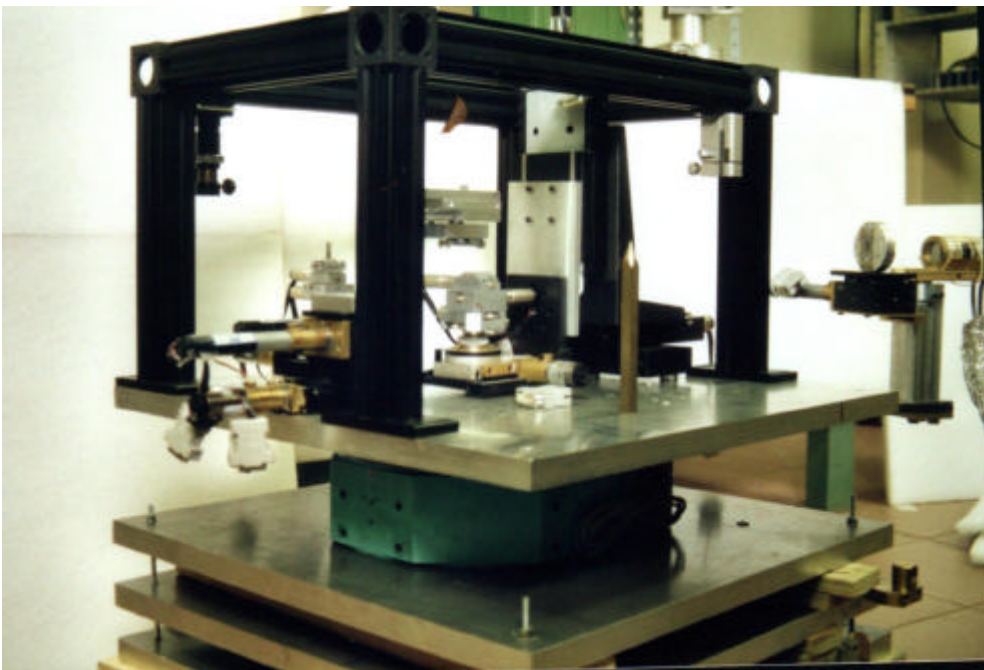


Figure 2.1: *Picture of the overall view of the instrument*

We therefore designed the new instrument with the following characteristics:

- i) It is specifically designed for microdiffraction experiments and all movements have a high degree of precision and accuracy.
- ii) it is transportable and suitable to be installed on many beamlines.
- iii) It is flexible and open to new improvements

- iv) It can be operated both by the software specific of ESRF (spec) and by a software running on any PC. This allows operation off-line. Therefore pre-alignment procedures can be done before installation on the beamline.
- v) The instrument can be interfaced to a laboratory x-ray source, therefore continuous improvements can be carried out on it and new alignment and experimental procedures can be tested without wasting synchrotron beam-time.

The diffractometer is composed of three main elements, visible in fig. 2.1 which gives an overall view of the instrument:

- 1) a base plate which consists of three aluminum plates; the bottomest (#1) is fixed and can be put on an adjustable table or alternatively can stand on three feet adjustable in height. On top of plate #1 another aluminum plate (#2) of the same size can slide with respect to plate #1 in the direction transverse to the x-ray beam. In between the two plates four small stainless steel platelets are embedded which reduce the friction. On top of plate #2 a third aluminum plate (#3) can rotate with respect to plate #2. The same kind of stainless steel platelets help the movement. Both the sliding and the rotation movements are acted by pushing screws and measured by comparators.
- 2) a goniometer which will hold the detector. It is firmly connected to plate #3 and its center of rotation coincides with the center of rotation of plate #3.
- 3) A fourth aluminum plate (#4) which holds the most important elements: an holder for the monochromator with 5 degrees of freedom (three motorised), an holder for the waveguide with six DOF (five motorised) and an holder for the sample with six DOF, all motorised. The plate #4 is connected directly to plate #3 through an aluminum cylinder, concentric with the goniometer.

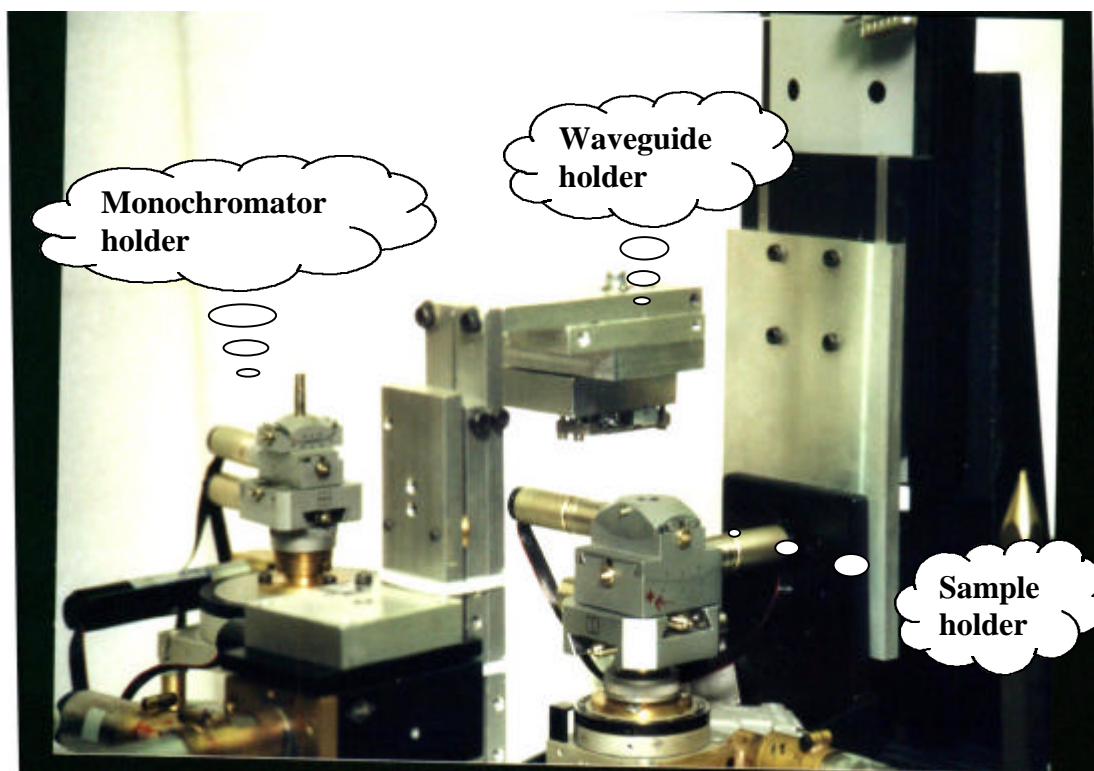


Figure 2.2: The picture shows the three main elements: the monochromator holder, the waveguide holder and the sample holder

An important feature in every diffractometer is that the center of rotation of sample and the center of rotation of detector coincide. In our case the sample holder can be moved in all the directions, and a pre-alignment procedure will bring the two centers to coincide. This procedure is carried out with the help of a stainless steel tip mounted in the center of rotation of goniometer (which in turn coincides also with the center of rotation of plate #3). As better described in the manual for use of the diffractometer, using two video cameras it is possible to bring the center of rotation of sample to coincide with the center of rot. of goniometer with an accuracy of the order of 100μ .

Fig. 2.2 shows the three main elements: the monochromator holder, the waveguide holder and the sample holder. For clarity reason we adopt a reference frame where X is the direction of the x-rays, Y is horizontal and transverse to X, and Z is vertical. θ_X , θ_Y and θ_Z are the rotations around the corresponding axes.

- i) **The monochromator.** The monochromator holder is constituted of a goniometer head (X, Y, θ_X and θ_Y) mounted on top of a goniometer (θ_Z). Only Y, θ_Y and θ_Z are motorised. The total angular range of θ_Z is 360° , but the range accessible with the motor is only few degrees. The monochromator is therefore roughly positioned manually, and its correct position refined with the motor. We used a Si channel-cut monochromator, shown in fig. 2.3. The incident beam is diffracted once by the first slab and then by the second. The beam diffracted twice is therefore parallel to the incident beam, and laterally displaced by the quantity $2g\cos\theta_B$, where g is the distance between the two slabs (gap) and θ_B the Bragg angle. For the channel cut shown in fig. 2.3 the gap is 1.8 mm. The Y movement has the purpose to properly position the first slab in the beam, while θ_Y controls that the diffraction takes place in the horizontal plane.



Figure 2.3: *The picture shows the Si channel-cut monochromator*

- ii) **The waveguide holder.** The waveguide holder is constituted of a home-made positioning arm for precise control of θ_Y and θ_Z , mounted on a X, Y and Z translation stage (see fig. 2.2). θ_Y is the most critical movement, because controls the angle of incidence of the incoming beam on the waveguide. As explained in del. D11 an intense beam exits from the waveguide only if the resonance condition (i.e. a correct angle of incidence) is met. The resonance is particularly narrow (few microrads) therefore the waveguide holder must have not only a very high angular resolution, but also a very good stability during the measurements. The angular range is quite limited (few degrees), therefore we choose a flexural pivot for both rotations. The advantage of the flex pivot with respect to a goniometer are the absence of friction and the intrinsic precision and accuracy. We assembled θ_Y and θ_Z in order to have the end of the waveguide on the intersection of the two axes of rotation. Among the three translations Z is the most critical, because from the vertical position depends the distance that the beam must travel inside the waveguide, and then the efficiency of the WG. The precision of Z should be of the order of few microns, but it is also very important that the angular deflection related to a displacement in Z (pitch and yaw) be kept as small as possible. The Y translation has the purpose to vary, transversely to the beam direction, the part of the WG probed by the beam. Finally, X changes the distance sample-WG. The last rotation, θ_X , is not motorised but is realised with a simple mechanical system composed of three screws and springs.
- iii) **The sample holder.** The sample holder is constituted of an X Y and Z stage which holds a goniometer and a goniometer head with 4 Degrees of Freedom (see fig. 2.2). Of these last the two translations are not motorised, but are needed to bring any part of the sample under examination on the center of rotation of the goniometer. An important step of the alignment procedure is to bring the center of rotation of the sample goniometer on the center of rotation of the detector arm (we define this axis as the center of rotation of the whole diffractometer). This operation is made with the help of two video cameras, as better explained in the diffractometer manual. The Z translation is constituted of a large translation stage mounted vertically. The precision and accuracy is better than 1 micron, and the minimum step is $6 \times 10^{-4} \mu$. Is therefore suitable to perform vertical scans with high spatial resolution. The other critical movement is the θ_Z rotation which is used to span the diffraction angle in the rocking curve, and is constituted of a high precision goniometer. θ_X and θ_Y are two movements used for the correct alignment: θ_X controls that the structures of interest lie in the horizontal plane, and θ_Y that the diffracting plane is horizontal. The other two translations, which are below the θ_Z goniometer, bring the part of the sample of interest in the x-ray beam. Care must be taken that the point of impact of the x-ray beam on the sample be always in the center of rotation of the diffractometer. This is insured by two video cameras.
- iv) **The detector goniometer.** The detector, shown in fig. 2.4, is carried by the large goniometer visible in fig. 2.1. A long stainless steel arm holds the detector, in this case a scintillator, and a slit holder for both horizontal and vertical slits. Slits with different, calibrated apertures can be used. The vertical position can be adjusted by means of a Z translation. This is important in order to select only the guided beam

and to hide the reflected and incident beams that arrive at the detector at different quotas, as explained in del D11 and in the alignment procedures. On the detector arm it is possible to mount also a CCD camera to perform measurements in the projection geometry.

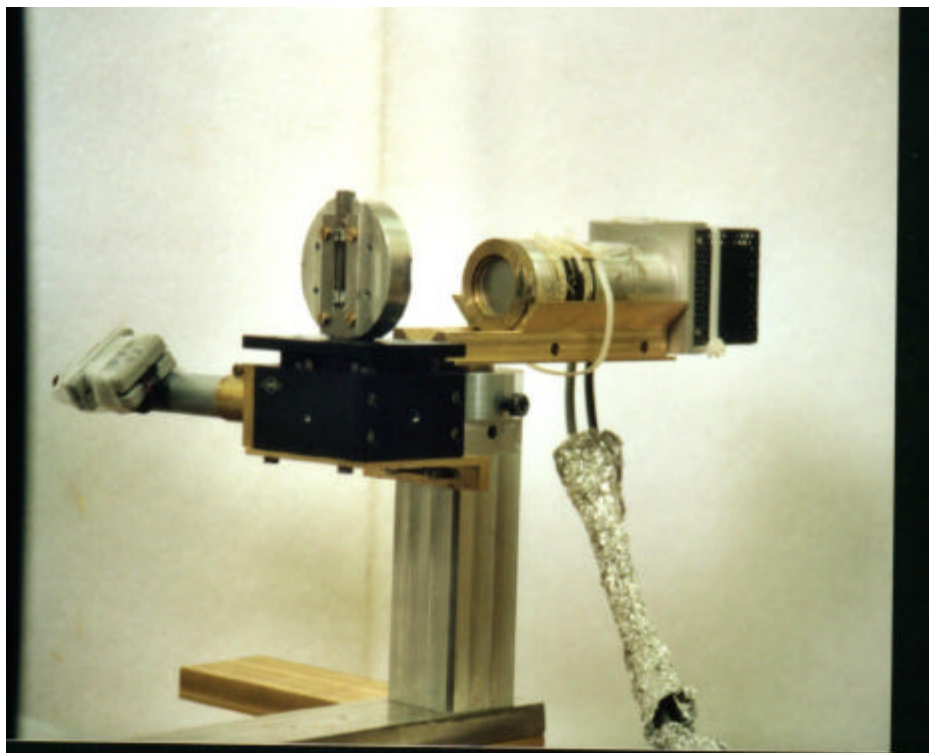


Figure 2.4: *Picture of the detector arm with the scintillator and the motorised slit system in front.*

- v) **The video cameras.** Two video cameras with enlarging optics that give an overall magnification of about a factor 40 are used to help in alignment and correct positioning. One camera controls from the top the distance between the waveguide and the sample, and once the calibration procedure is carried out, that the part of the sample in diffraction be in the center of rotation of diffractometer. The second camera, put horizontally, has the purpose to select the part of the sample to analyse. The video cameras are mounted on the frame visible in fig. 2.1.
- vi) **The linear transducers.** Two linear transducers of high sensitivity (0.3 and 1 μ) can be used to calibrate and control the movements. They can be mounted on different positions depending on needs.
- vii) **The motor control.** All the motors are d.c. motors with incorporated gear reduction mechanism and encoder. Each motor has its own motor control. Up to 16 motor controls can be connected in series and controlled by a RS232 port. For operation on the beamlines the motor controls have been integrated in SPEC, the software used at ESRF. For operation off-line its own software is available.

3) Software for data analysis

The software for data analysis is a very important part of the process which can give us information about the strain. In fact, as pointed out already in del. D11, the diffraction profile give us an integrated response of the whole volume probed by the x-rays. Therefore we have to face to an inverse problem, because we must extract from the diffraction profile the strain depth profile that produced the measured profile. This can be done by means of a fitting procedure, where a given structure, approximated by a stack of lamellae each with its own thickness and its own strain value, is considered and the resulting diffraction profile is calculated using the dynamical theory of diffraction. The diffraction profile is then compared with the measured one, and the deviation is calculated numerically. Then the strain and thickness of each lamella is modified in order to give the minimum χ^2 value. Since microdiffraction experiments, both in the projection and in the scanning geometry, would produce a great number of spectra, an automatic procedure should be set-up in order to improve the efficiency. The software has been elaborated by Cinzia Giannini and Antonietta Guagliardi of the Institute of Crystallography (IC) of CNR of Bari.

The program makes use of the dynamical theory (in the Takagi-Taupin recursive formalism) in order to calculate the diffraction profile of a lamellar structure and **FIT** the experimental x-ray data. Each lamella is characterized by its strain and thickness: $\epsilon_{zz}(\mathbf{i})$, $\mathbf{t}(\mathbf{i})$. The program must start with an initial sequence of lamellae that can be provided in two ways:

an external source (i.e. IMPACT, Finite Element model or analytical model) as a simple ASCII file *if the strain profile is known*

an initial guess given by the program itself as a consequence of a careful analysis of the experimental x-ray data *if the strain profile is completely unknown*.

The first step is to plot together sample data and blank data; here for blank data we mean the diffraction profile of an unstrained silicon crystal. This comparison allows us to estimate background and to fix markers in the angular range which will be used to extract the strain profile (initial guess).

The strain content of each lamella $\epsilon_{zz}(\mathbf{i})$ can be estimated by the distance $\theta_i - \theta_B$ according to the following relationship:

$$\epsilon_{zz}(\mathbf{i}) = -\cot g\theta_B (\theta_i - \theta_B)$$

where θ_B is the Bragg angle of the reflection chosen. In the following only the planes parallel to the surface will be considered, therefore only the ϵ_{zz} component of the whole strain tensor can be determined.

Due to minus sign in previous equation, the left hand side of the Bragg peak corresponds to tensile strain, the right hand side to compressive strain.

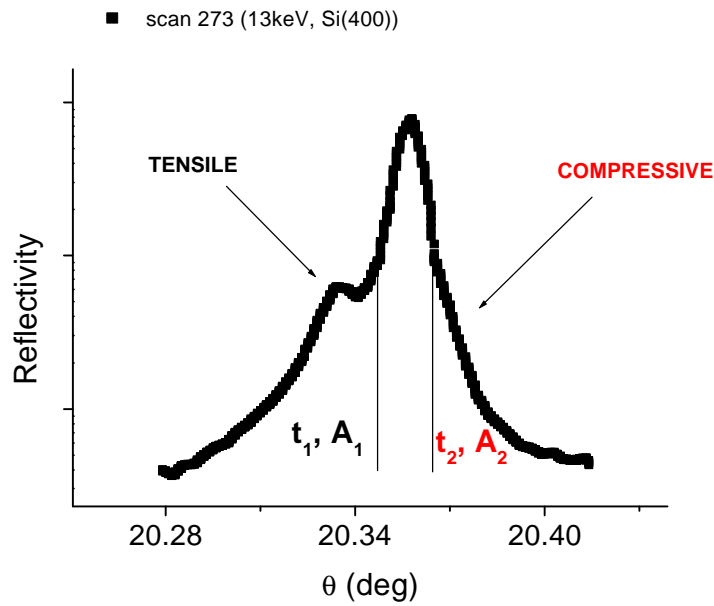


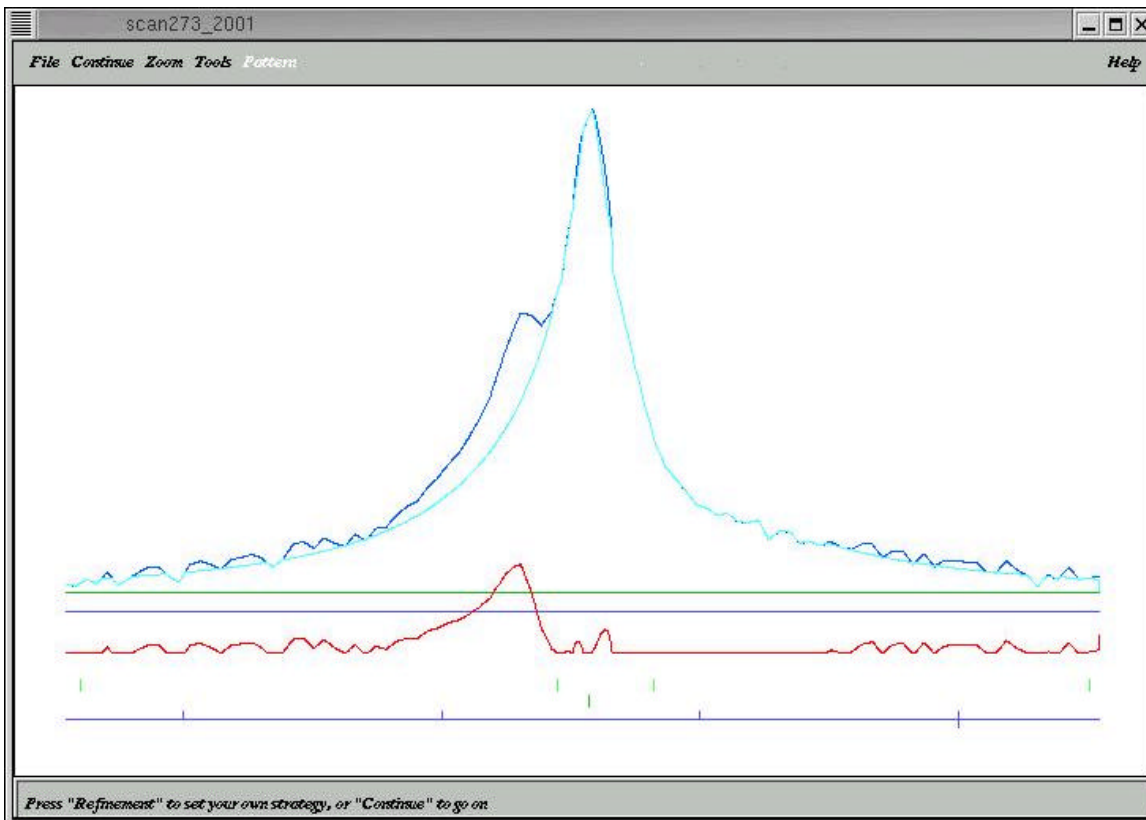
Figure 3.1: Example of a diffraction profile (in log scale) with indications of the compressive and tensile parts of the curve.

The other parameters to determine are the thickness of each lamella. This can be done following this simple procedure: the full area A_{tot} below the experimental blank profile (substrate included) corresponds to the extinction length ($t_{ext}=3.45 \mu\text{m}$ for Si(400) at $\lambda=0.95 \text{ \AA}$). The area below the tensile or compressive region A_1 or A_2 corresponds to a tensile or compressive length according to the simple relationship: $t_{ext}/A_{tot} = t_1/A_1 = t_2/A_2$. Then the contribution to the total intensity of each lamella of thickness $t(i)$ with tensile or compressive strain can be estimated by the corresponding intensity $I(i)$ normalized to t_{ext}/A_{tot} .

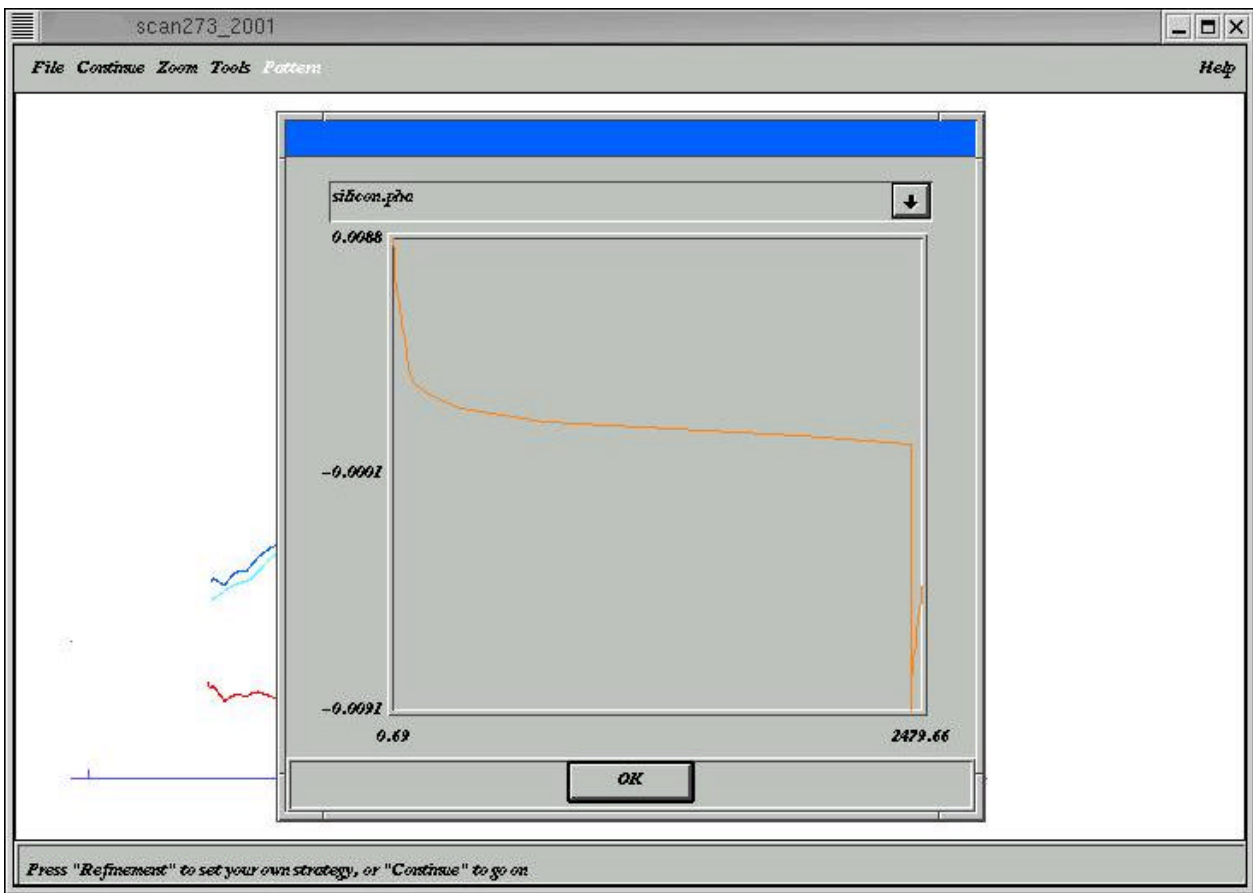
Fitting is extended to the full angular range, including the substrate peak. Therefore, an instrumental function is inserted and convoluted with the dynamically calculated x-ray data before the comparison with the experimental profile. Once the initial structure (strain and thickness of each lamella) has been determined ab-initio by the careful analysis of the experimental curve, the strain profile is refined by using a *trial&error* approach: random shifts are generated in a limited range of variation on the strain values $\epsilon_{zz}(i)$ as well as on the thickness $t(i)$ and the new values are kept or discarded following the principle of searching for the minimum of the χ^2 value corresponding to the best FIT.

In the following we resume the main steps of the program.

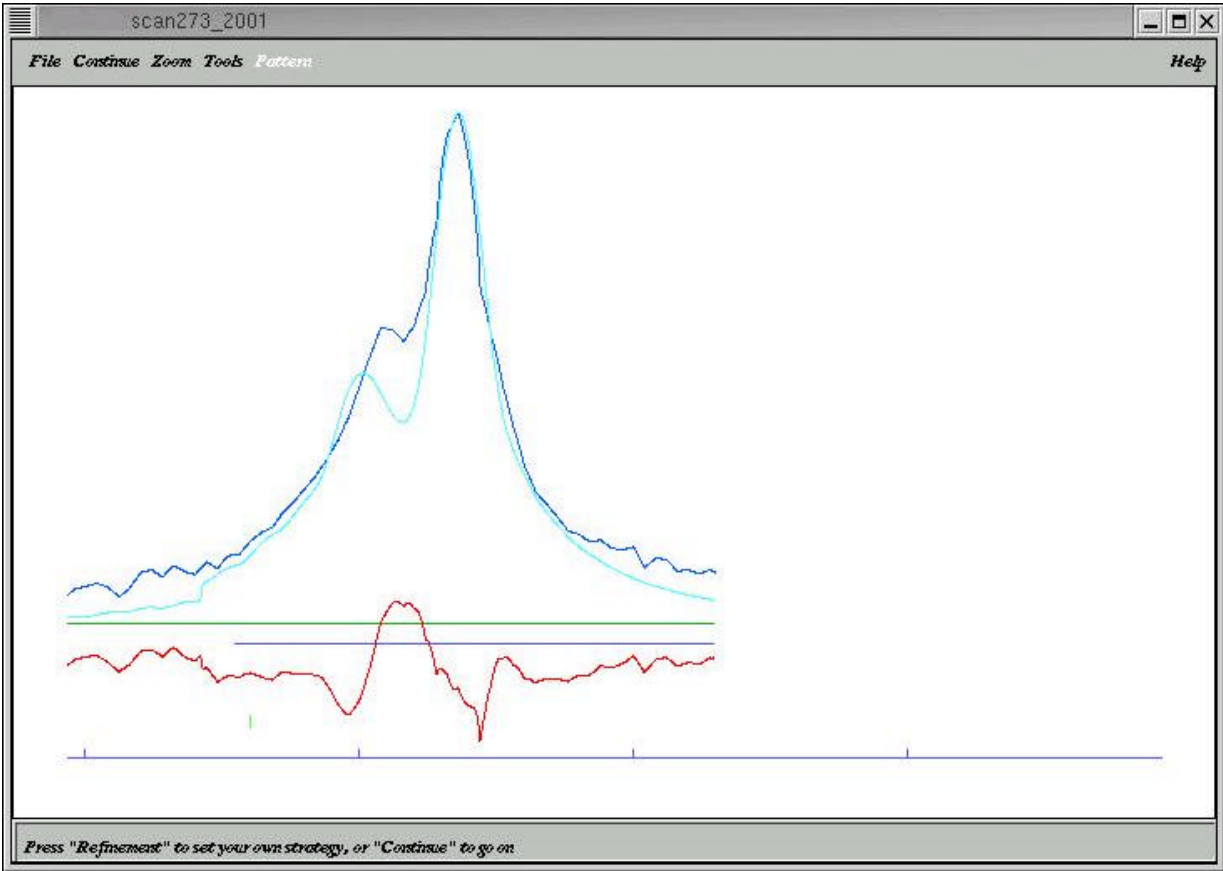
1. Plotting of the sample and blank data, together with the difference between the two



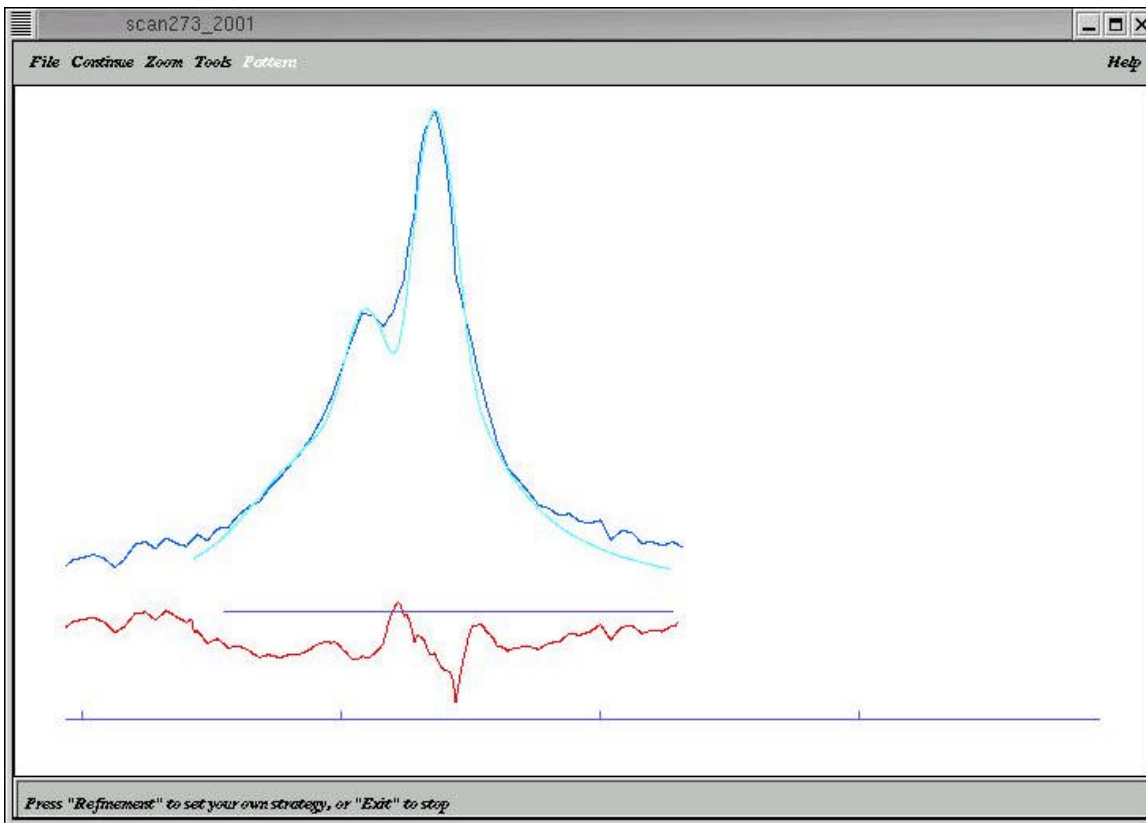
2. Initial strain as extracted from the experimental profile.



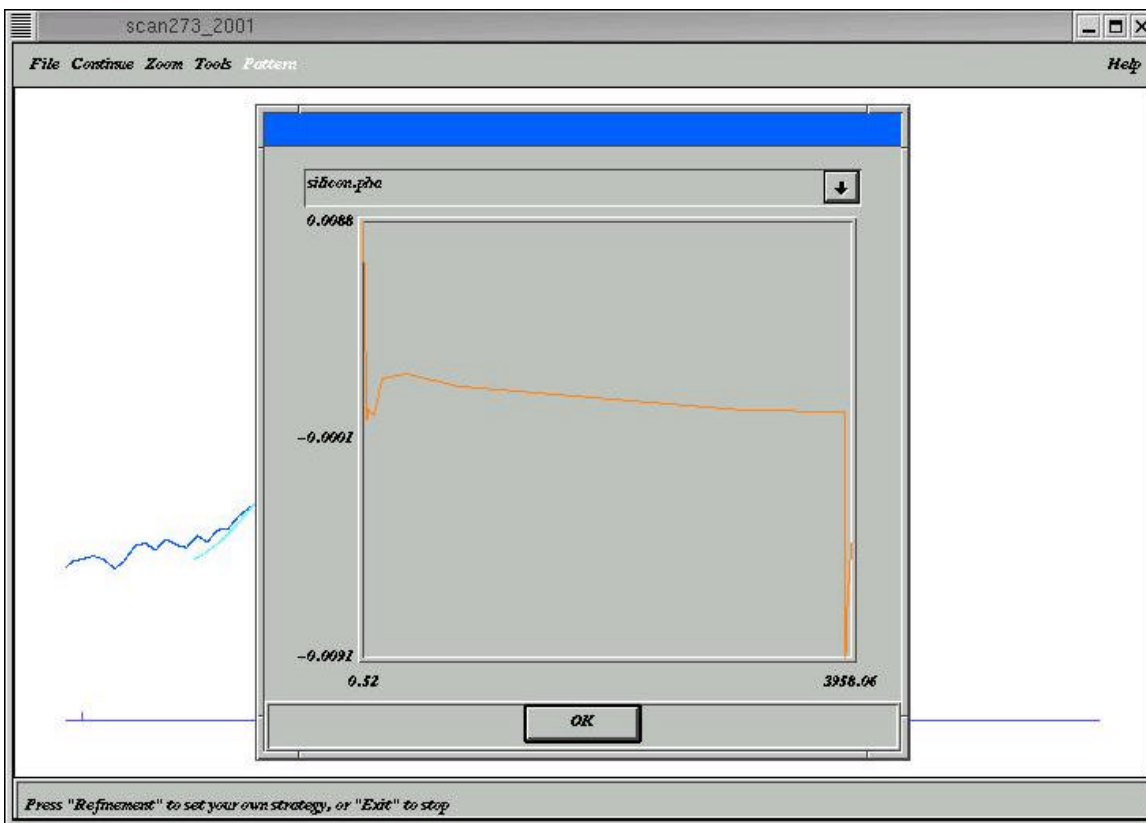
3. Dynamically calculated curve based on the strain profile extracted in step 2.



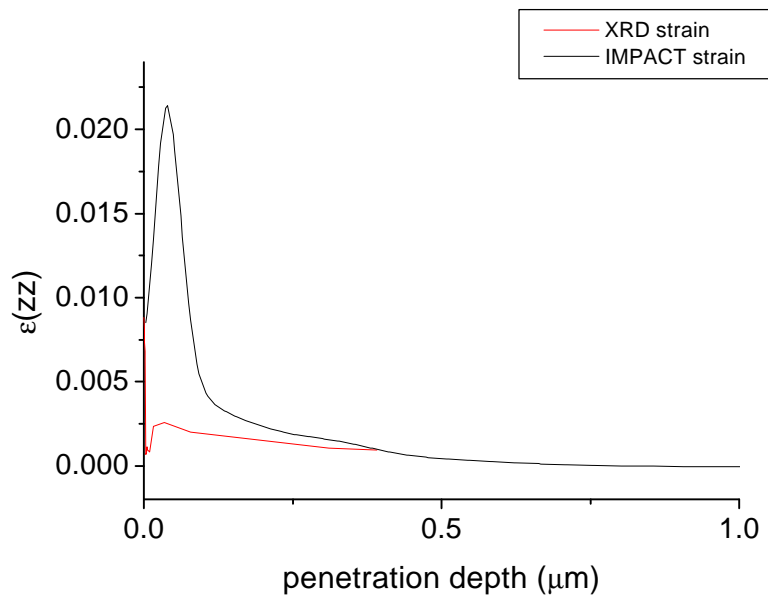
4. Final fit obtained after variation of strain and thickness.



5. Final Strain



Comparison with IMPACT.



It must be noted that the program is still in an optimization phase and is not ready to be distributed.

4) Results of measurements

In the course of the second year of activity we carried out four run of measurements at ESRF, two at a bending magnet beamline (BM5 in May 2001 and in February 2002), and two others at an undulator beamline (ID32 in Oct. 2001 and in March 2002).

In May 2001 we tested the non-dispersive geometry and the scanning mode. Useful data were taken on a sample of the second campaign (A044773_10).

In October 2001 we tested a first, very simplified version of the instrument described above, but we had very serious problems arising from instabilities of the beamline monochromator. Therefore that run didn't produce useful data.

In February 2002 we carried out measurements at BM5 using the beamline apparatus because our instrument was not available due to the improvements we had to perform on it. Also in this run we had to face instabilities due to some mechanical problems, not yet completely understood. In this run therefore only some refinement of the data taken in previous run could be possible.

In March 2002 the final version of the instrument was available. In this run two days were dedicated to measurement on STREAM samples and we decided to carefully analyse one sample of the first campaign.

As a result we will provide two examples of what can be obtained with the x-ray microdiffraction technique, one of the first and one of the second campaign. All the measurements were made using the (400) symmetric reflection, working at an x-ray energy of 13 KeV.

First campaign. Sample V004808

We made measurements on wafer #20 (HDP1 and HDP2, oxide annealing and 120 nm nitride). We analysed two structures, one (#4) with active zone $W = 0.22 \mu$ and space $S = 0.48 \mu$, and one (#5) with a more complex sequence: $a1=2, s1=6, a2=25, s2=3.5, a3=25, s3=6$ (measure in microns). The result for structure #4 is shown in fig. 4.1.

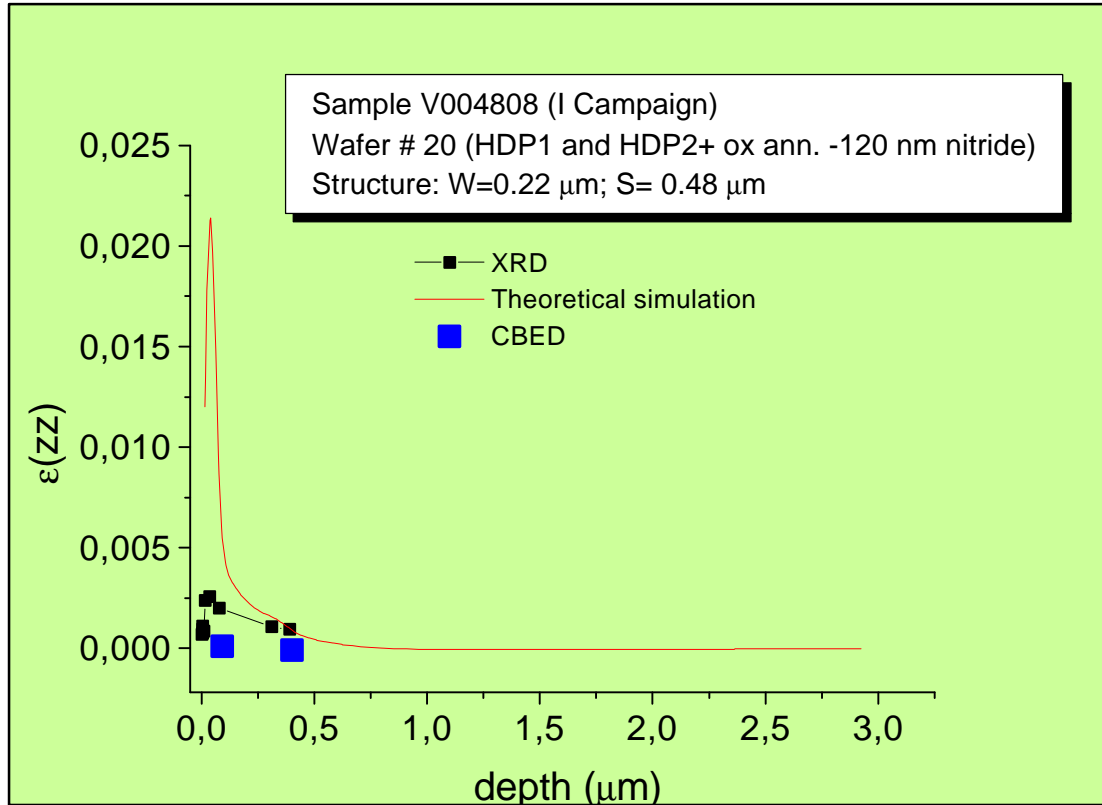


Figure 4.1: Strain result for XRD and comparison with CBED measurements and simulations for sample V004808_20_st_4.

A maximum strain of about 3×10^{-3} is measured, intermediate between the result of CBED and IMPACT simulations. With the spatial resolution of the scanning mode (about 0.3μ) we cannot distinguish between center and edge of the stripe.

The analysis of structure #5 is more complex because requires fitting on many rocking curves, and data analysis is not yet finished. It is interesting however to show a vertical scan at a fixed angle, indicative of the presence of strain.

Fig. 4.2 shows this vertical scan at an angle corresponding to a compressive strain of about -8×10^{-4} . A similar result is obtained for a tensile strain.

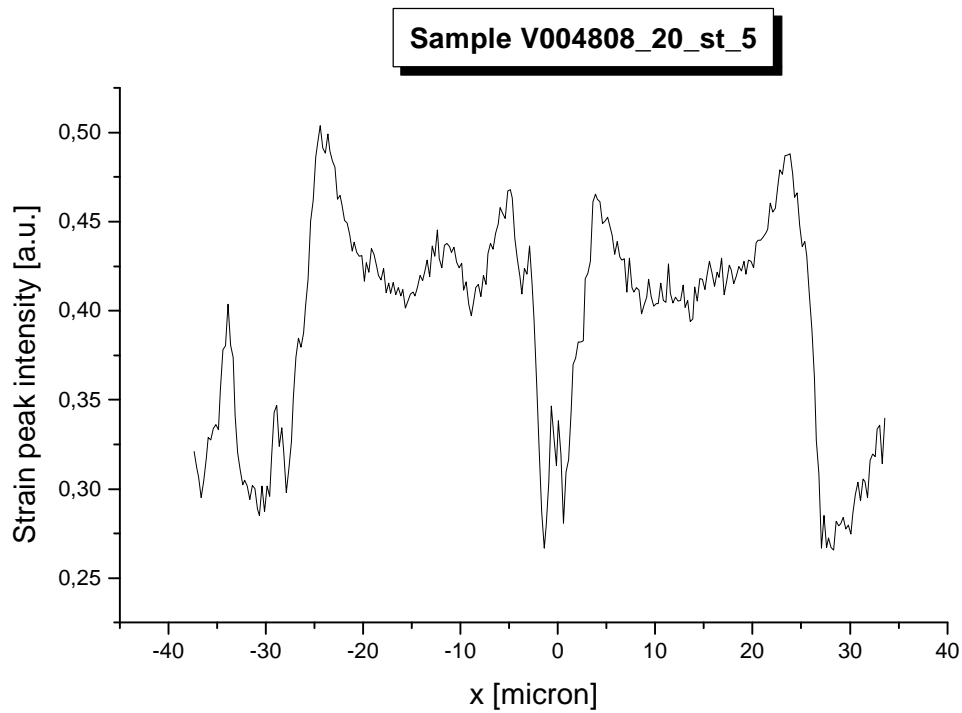


Figure 4.2: vertical scan of the structure #5 of sample V004808_20 at an angle corresponding to a strain of about -8×10^{-4}

This result roughly indicates that maximum strain and/or maximum volume interested to strain occurs at the edge of the active zone. It is interested to note that similar result has been found also from μ -raman measurements (see for ex. fig. 3.2.4 in del. D08). A careful analysis of the x-ray spectra will clarify if the strain increases or the volume interested to strain.

Second campaign. Sample A044773

The measurements were carried out on wafer #10 (30 nm Ti and 25 nm TiN). We took into consideration the structure with active zone 0.2μ and $S = 5 \mu$. Fig. 4.3 shows the XRD result together with comparison with CBED and simulations.

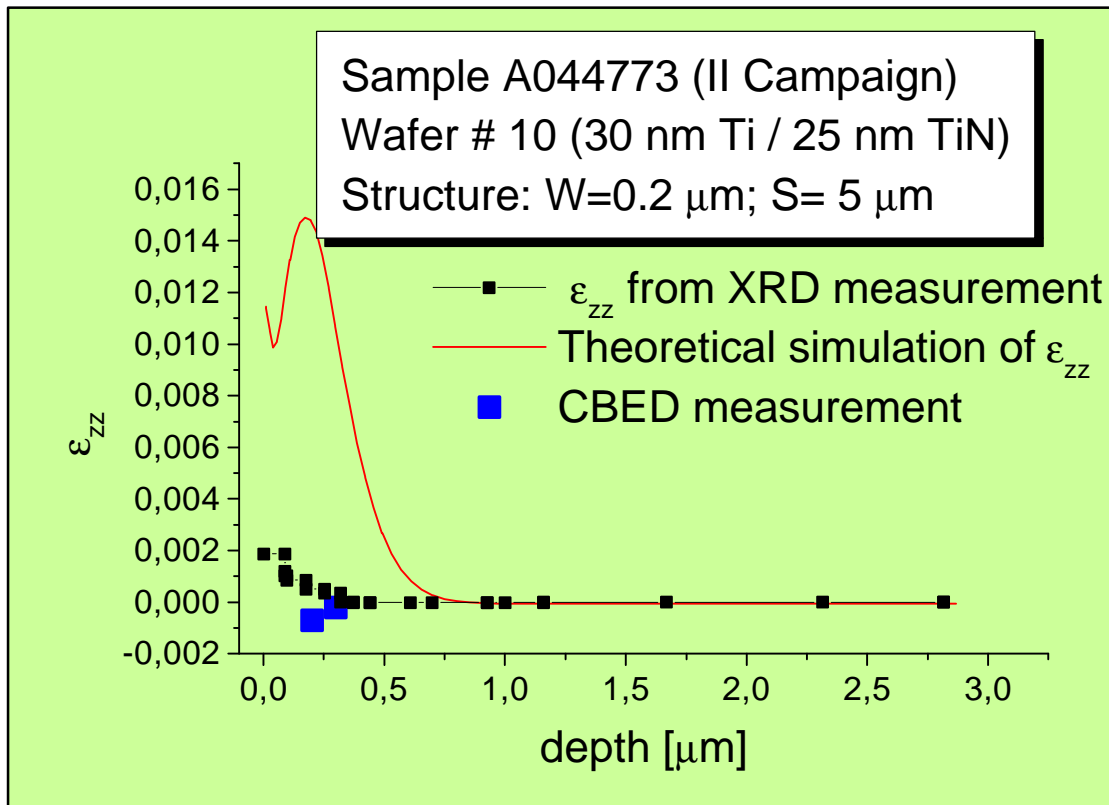


Figure 4.3: Strain result for XRD and comparison with CBED measurements and simulations for sample A044773_10. Structure $W=0.2$; $S=5$

Also in this case the XRD results are intermediate between the results of CBED and the IMPACT simulations. Quite similar results were found also for larger structures. One of the major problems is the correct positioning of the structure of interest in the beam. The alignment procedures, as described in the manual, can give an approximation of few microns. A more precise localization can take place considering the periodicity of the structures. For example, the structure related to fig. 4.3 has a periodicity of about 5μ . Fig. 4.4 shows a vertical scan at an angular position proper of a certain strain value (in this case about 2×10^{-4}). The periodicity is very well described and allows a precise localisation of the structure in the beam.

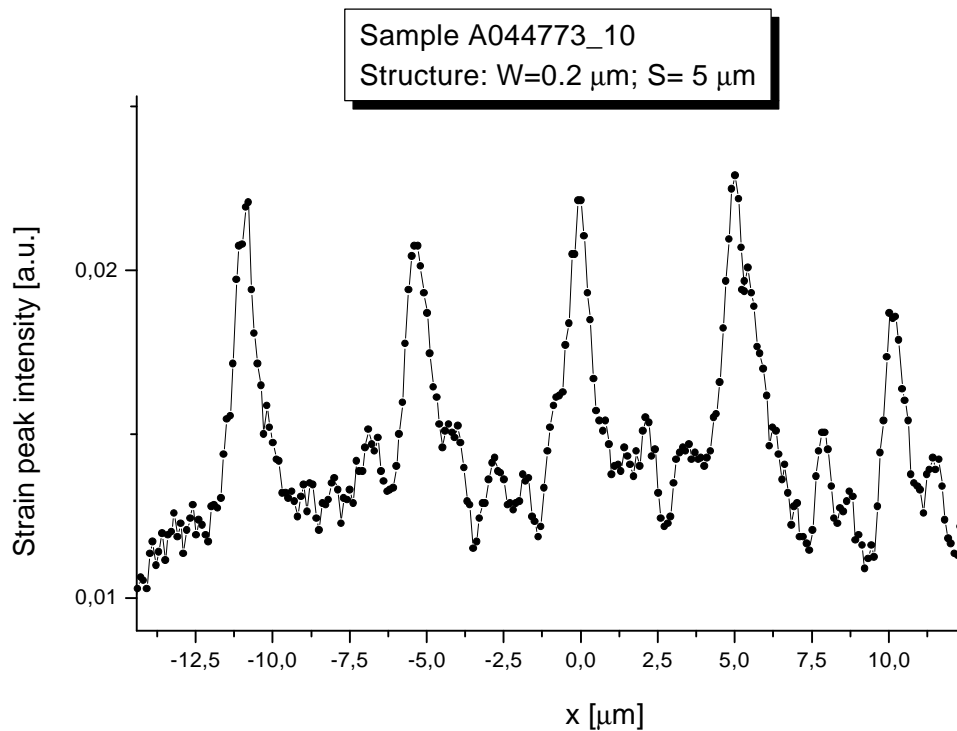


Figure 4.4: vertical scan of the structure $W=0.2$; $S = 5 \mu\text{m}$ of sample A044773_10 at an angle corresponding to a tensile strain of about 2×10^{-4}

A general comment about reliability of x-ray micro-diffraction results: a characteristic of x-ray diffraction is that, contrary to μRaman scattering, the strain value and the volume interested to strain can be determined independently. The strain value is extracted from the angular distance between the strain peak and the Bragg peak, the volume from intensity. Moreover, the theory underlying the reconstruction of the strain profile (the dynamical theory of diffraction) is very well established and reliable. However, a delicate point is the careful determination of background, mainly for shallow strained layers. If measurements are carried out properly the overall behaviour of the strain profile has a high degree of reliability.

5) Conclusions

This is the final deliverable related to the x-ray microdiffraction technique. We thanks the EU and all the partners of STREAM for the opportunity to improve this new technique applying it to a real problem and comparing the results with those obtained with other experimental techniques and simulations. In these two years of activity we learned a lot about the limits but also the unique features of the technique. These can be summarised in the following:

- i) from the experimental point of view is of paramount importance the mechanical and beam stability. The alignment procedures are quite complex and must be accomplished with the maximum accuracy. Any error will result in unusable data.
- ii) For reliable data the angular range must be as large as possible, the angular step as small as possible and the time acquisition as long as possible. These are evidently conflicting requirements, therefore a trade-off must be found together with proper data acquisition strategies (for example dividing the rocking curve in parts with different step-size and acquisition time).

- iii) The background should be as low as possible. Mainly for strain involving a shallow part of the sample a too high background can hinder the determination of the strain value. It is very important also to record the diffraction profile of an unstrained crystal.
- iv) The non-dispersive geometry gives a much narrower instrumental function, and this is important to enhance the sensitivity to strain.
- v) The projection mode is in principle better, because gives a better spatial resolution, but requires a very sensitive CCD detector with a high dynamic range. Alternatively the scanning mode can be used with a worse spatial resolution but the possibility to use any detector.
- vi) In spite of the complexity, we are convinced that the technique is worth to be pursued and improved because of its unique features. It is non-destructive, can be applied to any kind of materials and even to working devices (for example to measure strain or thermal expansion induced by current). Through the analysis of the rocking curve the entire strain depth profile can be reconstructed in a model independent way with sub-micrometer lateral spatial resolution.